Current Biology, Vol. 14, 1035–1046, June 22, 2004, ©2004 Elsevier Ltd. All rights reserved. DOI 10.1016/j.cub.2004.06.022

# MicroRNA Regulation of NAC-Domain Targets Is Required for Proper Formation and Separation of Adjacent Embryonic, Vegetative, and Floral Organs

**Allison C. Mallory,[1,4] Diana V. Dugas,[2,4] David P. Bartel,[1,3,*] and Bonnie Bartel[2,*]**
[1]Whitehead Institute for Biomedical Research
9 Cambridge Center
Cambridge, Massachusetts 02142
[2]Department of Biochemistry and Cell Biology
Rice University
6100 Main Street
Houston, Texas 77005
[3]Department of Biology
Massachusetts Institute of Technology
Cambridge, Massachusetts 02139

## Summary

**Background:** MicroRNAs (miRNAs) are ~21 nucleotide (nt) RNAs that regulate gene expression in plants and animals. Most known plant miRNAs target transcription factors that influence cell fate determination, and biological functions of miRNA-directed regulation have been reported for four of 15 known microRNA gene families: miR172, miR159, miR165, and miR168. Here, we identify a developmental role for miR164-directed regulation of NAC-domain genes, which encode a family of transcription factors that includes *CUP-SHAPED COTYLEDON1* (*CUC1*) and *CUC2*.

**Results:** Expression of a miR164-resistant version of *CUC1* mRNA from the *CUC1* promoter causes alterations in *Arabidopsis* embryonic, vegetative, and floral development, including cotyledon orientation defects, reduction of rosette leaf petioles, dramatically misshapen rosette leaves, one to four extra petals, and one or two missing sepals. Reciprocally, constitutive overexpression of miR164 recapitulates *cuc1 cuc2* double mutant phenotypes, including cotyledon and floral organ fusions. miR164 overexpression also leads to phenotypes not previously observed in *cuc1 cuc2* mutants, including leaf and stem fusions. These likely reflect the misregulation of other NAC-domain mRNAs, including *NAC1*, *At5g07680*, and *At5g61430*, for which miR164-directed cleavage products were detected.

**Conclusions:** These results demonstrate that miR164-directed regulation of *CUC1* is necessary for normal embryonic, vegetative, and floral development. They also show that proper miR164 dosage or localization is required for separation of adjacent embryonic, vegetative, and floral organs, thus implicating miR164 as a common regulatory component of the molecular circuitry that controls the separation of different developing organs and thereby exposes a posttranscriptional layer of NAC-domain gene regulation during plant development.

*Correspondence: bartel@rice.edu (B.B.), dbartel@wi.mit.edu (D.P.B.)
[4]These authors contributed equally to this work.

## Introduction

MicroRNAs are small regulatory RNAs (for review, see [1]) that were first discovered in animals [2–6] and more recently found in plants [7–9]. In animals, miRNAs are processed from imperfectly paired stem-loop precursor RNAs of approximately 70 nt, and some of the mature 21 nt miRNAs are reported to pair with target mRNAs to specify posttranscriptional repression of these targets [2, 3, 10–15].

In plants, miRNAs also derive from imperfectly paired stem-loops; however, these predicted precursors appear more variable in length than animal miRNA stem-loop precursors [7, 16]. Plant miRNA accumulation requires the nuclear activity of the RNaseIII DICER-LIKE 1 (DCL1) and to a lesser degree HEN1 and HYL1, nuclear-localized proteins with double-stranded RNA binding domains [7, 9, 17–20]. In addition, proper miRNA function requires AGO1 [21, 22], a protein with PAZ and PIWI domains that is conserved in most eukaryotes [23]. Like animal miRNAs, the accumulation of many plant miRNAs is not ubiquitous but, instead, varies in different organs and tissues and at different developmental stages, indicating that miRNA accumulation is spatially and temporally regulated [7, 8]. In addition, many of the miRNAs isolated from the dicot *Arabidopsis* are conserved in the monocot rice and other plant species, implying conserved evolutionary roles for plant miRNAs [7, 16, 24].

Many regulatory targets of plant miRNAs have been confidently predicted based on their extensive, evolutionarily conserved complementarity to the miRNAs [25]. Of the 15 miRNA families identified thus far in plants, all have at least one predicted mRNA target, and most are predicted to target multiple mRNAs [7–9, 25–27]. Experimental data, often the detection of an mRNA fragment diagnostic of miRNA-directed cleavage, have confirmed the identities of targets for 11 miRNA families [19, 26–32]. These data also support the idea that most plant miRNAs act within an RNA-induced silencing complex (RISC) to direct cleavage of their target messages, although in one case diminution of target protein without a corresponding reduction in target mRNA indicates that plant miRNAs can also act to inhibit productive translation [31, 32].

Plant miRNAs have a striking propensity to target messages encoding transcription factors involved in cell fate determination [25]. Consistent with the prediction that miRNA pathways regulate plant development, plant mutants defective in miRNA accumulation, such as *dcl1*, *hen1*, *hyl1*, and *ago1*, exhibit pleiotropic developmental phenotypes including floral development defects and leaf morphology alterations [19–22, 33–35]. The importance of this regulation is underscored by the observation that *dcl1* null mutations confer embryo lethality [36]. In addition, plants expressing a viral protein that alters miRNA accumulation and activity have developmental defects [29, 37]. Specialized developmental functions of specific plant miRNA families have recently been reported for the miR172, miR159/JAW, and miR165/166; these func-

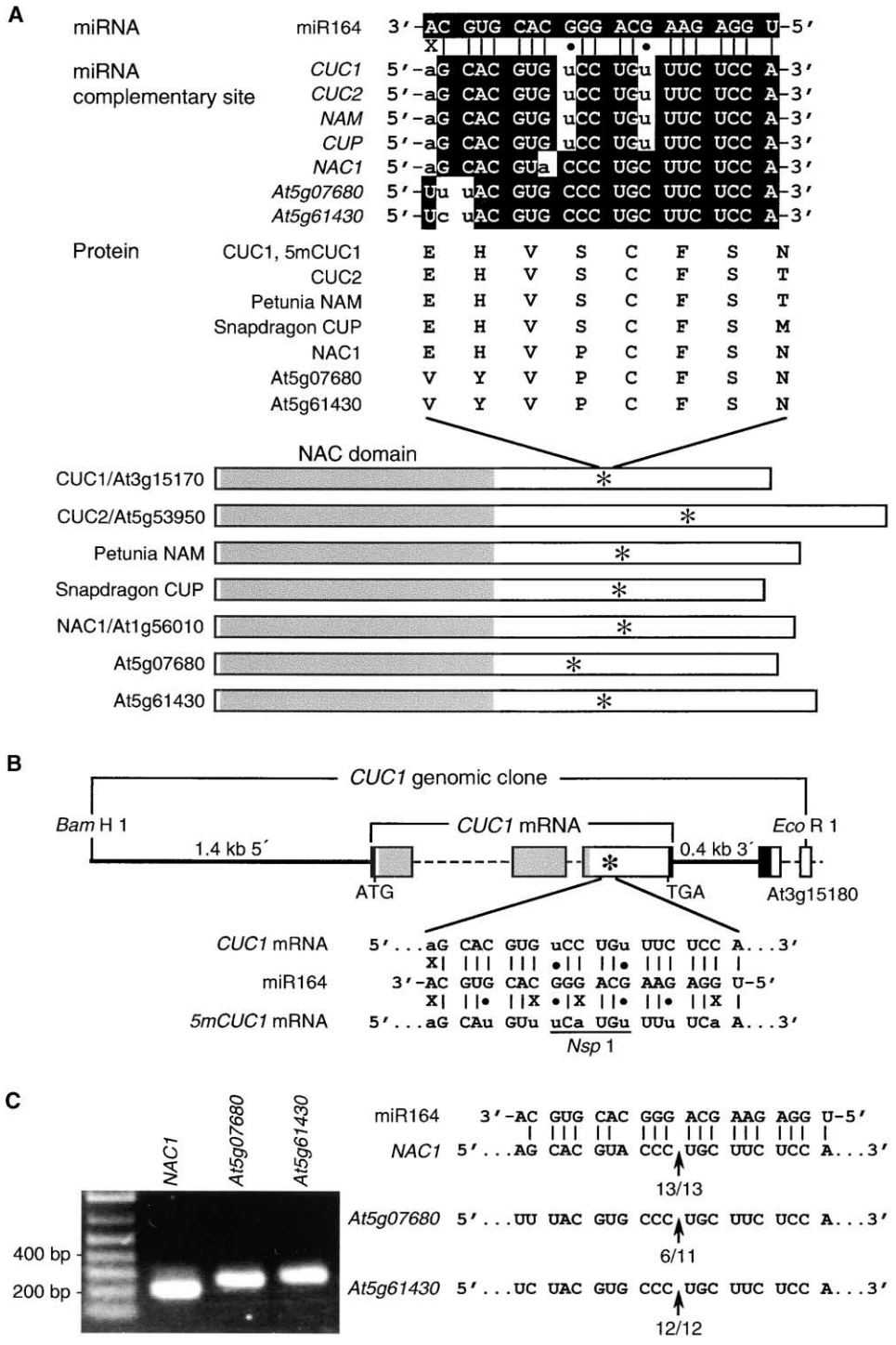


Figure 1. miR164 Complementary Sites in Plant NAC-Domain Genes

(A) Predicted pairing between miR164 and the miR164 complementary sites of *Arabidopsis* mRNAs *CUC1, CUC2, NAC1, At5g07680*, and *At5g61430* and of the petunia *NAM* (GenBank accession X92205) and snapdragon *CUC* (GenBank accession AJ568269) mRNAs. Watson-Crick base pairing between the mRNA and miR164 is indicated by black boxes, whereas mismatches and G:U wobbles are unshaded. Mismatches and G:U wobbles with *CUC1* are indicated by an X or black circles, respectively. The protein sequence encoded by the miR164 complementary site of each mRNA is listed. The open reading frames of each predicted miR164-target are depicted (rectangle), showing the position of each conserved NAC domain (gray box) and miR164 complementary site (asterisks).

(B) Illustration of the *CUC1* genomic clone used to transform *Arabidopsis*. Locations of the intergenic sequences (solid lines), intron sequences (dashed lines), 5′ and 3′UTRs (black boxes), NAC domain (gray boxes), remainder of the *CUC1* open reading frame (open boxes), start codon (ATG), stop codon (TGA), and miR164 complementary site (asterisk) are all indicated. Positions of the BamH1 and EcoR1 sites used for cloning and the downstream gene *At3g15180* are also shown. Messenger RNA segments from *CUC1* and *5mCUC1* are shown paired with miR164, with the Nsp1 restriction site unique to *5mCUC1* indicated.

(C) miR164 cleavage sites in *At5g61430, At5g07680*, and *NAC1* mRNAs determined by RNA ligase mediated 5′ RACE. At the left is the agarose gel showing the nested PCR products that were cloned and sequenced for each gene. At the right, the frequency of 5′ RACE clones corresponding to each cleavage site (arrows) is shown as a fraction, with the number of clones matching the target message in the denominator.

tions include roles in flowering time and floral organ identity [31, 32], rosette leaf curvature [26], and organ polarity [21, 38, 39], respectively. Two miRNAs, miR162 and miR168, are likely to influence development through feedback regulation of the miRNA pathway itself [22, 27].

miR164 is potentially transcribed from two loci, *MIR164a* and *MIR164b* [7], and is predicted to target a subset of genes in the NAC-domain transcription factor gene family [25]. This family, named after the founding members, petunia *no apical meristem* (*NAM*), *Arabidopsis ATAF1* and *ATAF2*, and *Arabidopsis CUP-SHAPED COTYLEDON2* (*CUC2*) [40, 41], is restricted to plants and has more than 100 members in *Arabidopsis* [42]. Five *Arabidopsis* NAC-domain messages have a miR164 complementary site with three or fewer mismatches to miR164 (Figure 1A) [25]. These include *NAC1*, *CUC1*, *CUC2*, *At5g07680*, and *At5g61430*. The miR164 complementary sites are located in the last exon of the mRNAs, downstream of the conserved NAC domain [25]. Of these predicted miR164 targets, *CUC1* and *CUC2* mRNAs have been shown to be cleaved within the miR164 complementary site [29].

Of the five *Arabidopsis* NAC-domain genes with miR164 complementarity sites, three have established roles in development. *cuc1 cuc2* double mutants display defects in shoot apical meristem (SAM) formation as well as in cotyledon, sepal, and stamen separation [40, 43], revealing roles for *CUC1* and *CUC2* in both embryonic and floral development. These defects are weak and incompletely penetrant in single *cuc1* and *cuc2* mutants, suggesting some functional redundancy between *CUC1* and *CUC2* [40]. Plants expressing *CUC1* driven by the strong, constitutive 35S cauliflower mosaic virus (CaMV) promoter (*35S:CUC1*) develop lobed cotyledons and fused rosette leaves and display adventitious shoots on the adaxial surface of cotyledons and less frequently on the surface of rosette leaves [43, 44]. Plants expressing antisense *NAC1* under the control of the 35S promoter have reduced levels of endogenous *NAC1* transcript and display reduced lateral root emergence, whereas *35S:NAC1* plants have large leaves, thick stems, and increased numbers and length of lateral roots [45]. Thus NAC-domain genes with miR164 complementarity sites have been implicated in embryonic, vegetative, and floral development, but the significance of miRNA-directed regulation of these genes has not been explored.

Here, we report biological roles for miR164-directed regulation of target NAC-domain transcription factor mRNAs. *Arabidopsis* plants transformed with a miR164-resistant version of the *CUC1* target display embryonic, vegetative, and flower organ defects, including cotyledon orientation defects, rosette leaf abnormalities, and sepal and petal number and positioning defects. Furthermore, plants ectopically expressing miR164 exhibit cotyledon and floral organ fusion phenotypes overlapping with *cuc1 cuc2* double mutant defects [40]. These plants exhibit additional organ fusion phenotypes that likely result from the misregulation of other miR164 targets. Indeed, we detect mRNA fragments diagnostic of miR164-directed cleavage of *NAC1*, *At5g07680*, and *At5g61430* in wild-type plants. Together, these results identify a role for miR164-directed regulation and show

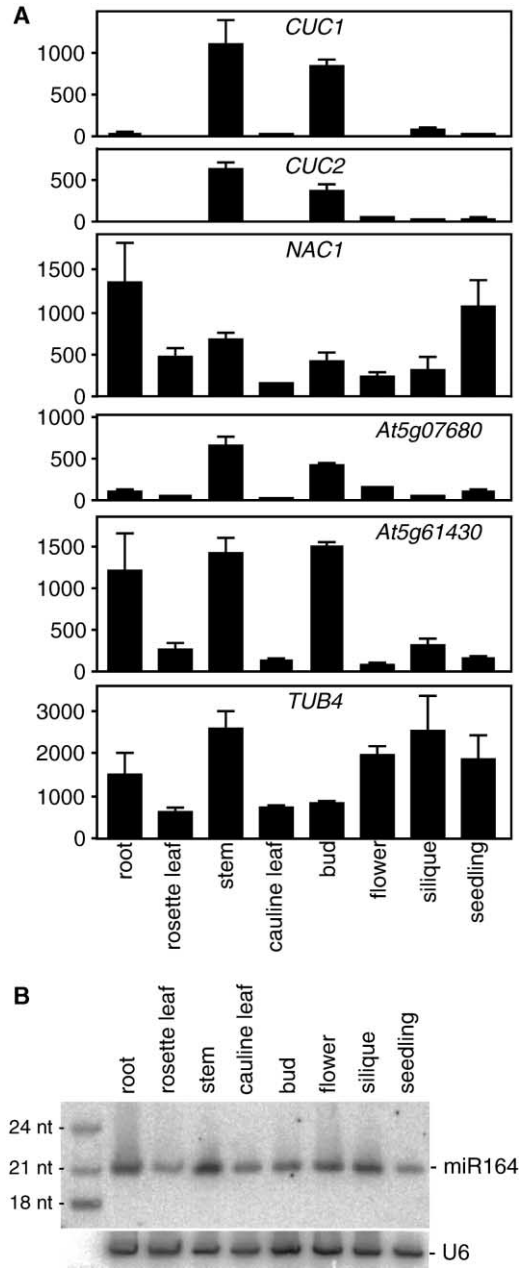


Figure 2. Accumulation of miR164 and miR164-Targeted NAC-Domain mRNA in *Arabidopsis* Tissues

(A) miR164 target mRNAs accumulate differentially in *Arabidopsis* tissues. The indicated NAC-domain mRNAs were quantified in total RNA prepared from root, rosette leaf, stem, cauline leaf, bud (includes a mix of buds and inflorescence meristems), flower, silique (includes embryonic tissues), and 12-day-old seedling tissues by using quantitative real-time RT-PCR with primers and probes designed around the miRNA complementarity sites and normalized to the level of 18S rRNA in the sample. *TUB4* was used as a nontarget control. mRNA levels are displayed in arbitrary units, and error bars represent the standard deviations of three PCR replicates of a single reverse transcription reaction.

(B) miR164 accumulates differentially in *Arabidopsis* (Col-0) tissues. RNA gel-blot analysis of 30 μg RNA from (A) with a DNA probe complementary to miR164. The positions of $^{32}$P-labeled RNA oligonucleotides are noted on the left. The blot was stripped and reprobed with an oligonucleotide complementary to U6 as a loading control.

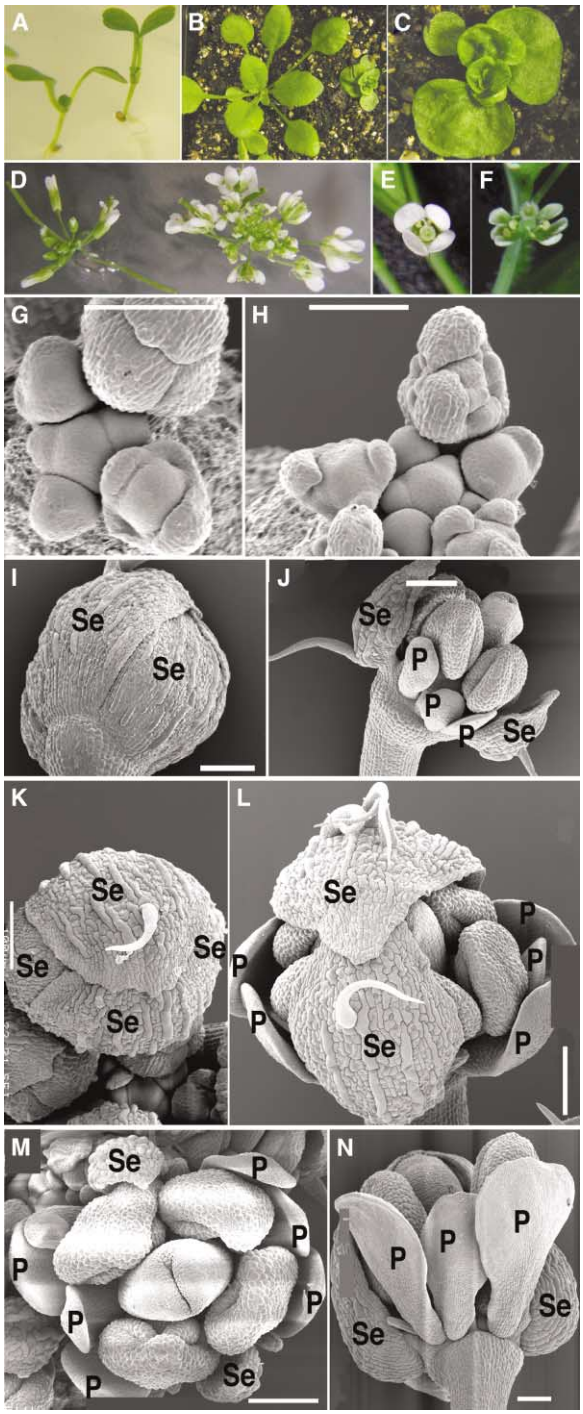


Figure 3. Developmental Abnormalities in *5mCUC1* Plants

(A–C) Vegetative development of *5mCUC1* plants and control *CUC1* plants. (A) 10-day-old T2 control *CUC1* (left) seedling with wild-type phenotype and *5mCUC1* (right) seedling with upright cotyledon petioles. (B) 23-day-old T2 control *CUC1* (left) and *5mCUC1* (right) plants. (C) Magnified view of a 23-day-old T2 *5mCUC1* plant.

(D–N) Comparison of floral organs of representative control *CUC1* plants and *5mCUC1* plants. Vertical views of a T1 control *CUC1* (left) and *5mCUC1* (right) floral apex (D). Vertical views of a control *CUC1* T1 flower with four petals and four sepals (E) and a *5mCUC1* T1 flower with six petals and two sepals (F). Scanning electron micrographs (SEM) of a T2 control *CUC1* (G) and a *5mCUC1* (H) inflorescence. Note the altered number and position of developing sepals in *5mCUC1*. Horizontal view SEM of T2 control *CUC1* (I) and *5mCUC1* (J) floral buds and vertical view SEM of T2 control *CUC1* (K) and *5mCUC1* (L) stage-12 flowers. Note the absence of a sepal pair in the *5mCUC1* buds causes buds to open. Vertical view SEM of a young T2 *5mCUC1* flower (M) and horizontal view SEM of a more mature *5mCUC1* flower (N). Petals (P) and sepals (Se) are indicated. Scale bars = 100 μm.

that proper miR164-directed regulation of NAC-domain genes is essential for normal plant morphogenesis.

## Results and Discussion

### A miR164-Resistant Version of *CUC1* Alters Embryonic, Vegetative, and Floral Development

*CUC1* mRNA is found in most tissues assayed [43], whereas *CUC2* mRNA is most abundant in flowers and seedlings [43], and *NAC1* mRNA accumulates to the highest level in roots [45]. We used quantitative RT-PCR to compare mRNA levels of these three miR164 targets to each other and to additional predicted miR164 targets encoded by *At5g07680* and *At5g61430*. All five genes were highly expressed in stems and buds but differentially expressed in other organs and seedlings (Figure 2A). *NAC1* was highly expressed in roots and seedlings, and *At5g61430* expression also was high in roots. RNA blot analysis indicated that miR164 accumulates in all organs and developmental stages analyzed (Figure 2B), raising the prospect that it could be modulating the expression of these messages in many tissues of the plant.

To examine the importance of miRNA-directed regulation of CUC1, we constructed a miR164-resistant version of *CUC1 (miR-resistant CUC1*, *5mCUC1)* by introducing five silent mutations within the miR164-complementarity domain of a *CUC1* genomic clone, thus increasing the number of mismatches between the *CUC1* RNA and miR164 from three in wild-type to eight in *5mCUC1* (Figure 1B). These five mutations interrupt the potential for Watson-Crick base pairing between miR164 and *CUC1* without altering the amino acid sequence of the encoded CUC1 protein (Figure 1A). The introduced mutations also create an Nsp1 restriction site that allowed us to specifically monitor *5mCUC1* expression in plants.

We used an in vitro assay that relies on miRNA-programmed RISC endogenously present in wheat-germ extract [30] to determine whether miR164-directed cleavage of *5mCUC1* RNA is reduced. Specific cleavage was detected for the wild-type (wt) *CUC1* RNA, but not for the *5mCUC1* RNA (data not shown), although in both cases most of the RNA remained uncleaved after a 60 min incubation, suggesting that these extracts have only low levels of miR164-programmed RISC or perhaps that the sequence of this miRNA has diverged in wheat.

To assess the in vivo consequences of disrupting miR164 regulation of *CUC1*, we transformed wt *Arabidopsis* plants with *5mCUC1* and control *CUC1* genomic constructs under the control of the native *CUC1* 5′ and 3′ regulatory sequences (Figure 1B) and analyzed the resultant transformants for developmental defects. None of the 62 control *CUC1* primary transformants displayed any morphological abnormalities. In contrast, 34 of 74 *5mCUC1* transformants displayed striking floral organ phenotypes that included one to four extra petals and one or two missing sepals (Figures 3D–3F); these pheno-

types were observed in *5mCUC1* progeny as well (Figures 3G–3N). In wt plants, petals and reproductive structures are encased within two pairs of sepals as buds develop (Figures 3G, 3I, and 3K). In *5mCUC1* plants, the altered sepal number and position, delayed sepal formation or maturation, and the proliferation of petal organs caused immature floral buds to expose petals and reproductive structures throughout development (Figures 3H, 3J, and 3L–3N). Moreover, mature flowers of *5mCUC1* plants appeared larger than wt because of their open, claw-like shape (Figures 3E and F). Although floral organ development was altered in the *5mCUC1* plants, flower phyllotaxy on the primary stem and branches appeared normal. *5mCUC1* plants had reduced fertility compared to the control *CUC1* plants; however, all but the most severely affected plants produced viable seed, indicating that both male and female reproductive structures were at least partially functional.

In addition to the abnormal flower morphology, the progeny of some *5mCUC1* transformants displayed cotyledon orientation defects and rosette leaf abnormalities, including severe reduction of rosette leaf petioles and broadened rosette leaf shape (Figures 3A–3C). The *5mCUC1* progeny that exhibited rosette leaf abnormalities had the most severely altered floral organ development. Quantitative RT-PCR analysis revealed that floral buds and meristems of *5mCUC1* plants with aberrant phenotypes accumulate higher steady-state levels of *CUC1* mRNA than do those of *5mCUC1* plants with wild-type phenotypes, control *CUC1* plants, or untransformed wt plants (Figure 4A). In addition, the fraction of *CUC1* RT-PCR product that corresponded to *5mCUC1*, as monitored by Nsp1 digestion, correlated with the presence of the phenotype (Figure 4B). We also found that miR164 accumulation was unchanged in *5mCUC1* and control *CUC1* plants (data not shown), indicating that the expression of an additional copy of *CUC1* or *5mCUC1* does not affect miR164 biogenesis.

Because abnormal phenotypes were not observed in any of the 62 control *CUC1* primary transformants or progeny plants analyzed, we conclude that the *5mCUC1* phenotypes result from disruption of miR164-directed *CUC1* regulation rather than from simply expressing an extra copy of *CUC1* from endogenous regulatory elements. Together, the phenotypic and molecular data demonstrate that proper miR164-directed regulation of *CUC1* is essential for normal embryonic, vegetative, and floral organ development.

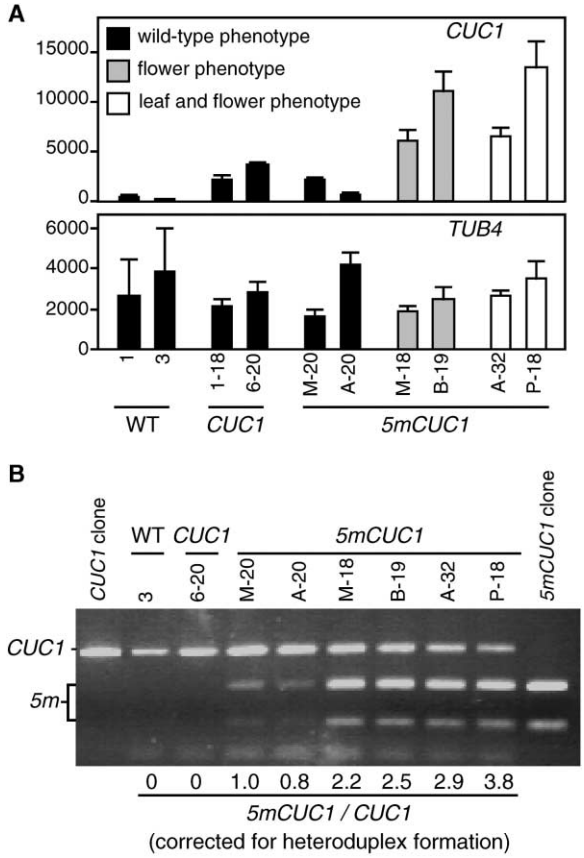


Figure 4. *CUC1* mRNA in *5mCUC1* Flowers

(A) Phenotypic *5mCUC1* plants accumulate increased steady-state levels of *CUC1* mRNA. The indicated mRNAs were analyzed by using real-time quantitative RT-PCR with primers and probes designed around the miRNA complementarity site of *CUC1* and normalized to the level of 18S rRNA in the sample. Total RNA was prepared from a mix of buds and inflorescence meristems of wt Col-0 plants, control *CUC1* 1-18 and 6-20, and *5mCUC1* M-20 and A-20 transformants lacking phenotypes, *5mCUC1* M-18 and B-19 transformants displaying flower phenotypes, and *5mCUC1* A-32 and P-18 transformants displaying both rosette leaf and flower phenotypes. *TUB4* is included as a nontarget control. mRNA levels are displayed in arbitrary units, and error bars represent the standard deviations of three PCR replicates.

(B) Relative levels of *CUC1* and *5mCUC1* mRNAs in transgenic plants. The same RNA used in (A) was reverse transcribed, and the resulting cDNA was PCR amplified to completion, then digested with Nsp1, which cuts the *5mCUC1* amplicon, but not the *CUC1* amplicon (Figure 1C) or heteroduplex molecules that result from annealing of *CUC1* and *5mCUC1* strands. Agarose-gel separation and ethidium-bromide staining revealed the full-length PCR product (330 bp) and the Nsp1 digestion fragments (220 bp and 110 bp). DNA gel-blot analysis (not shown) was used to quantitate the 330 bp and 220 bp DNAs, and the amount of *5mCUC1* relative to *CUC1* (correcting for heteroduplex) is shown below each lane.

### *mir164b* Mutant Plants Have Reduced miR164 Accumulation but Retain Sufficient miR164 to Prevent Developmental Abnormalities

Mutant plants that do not express miR164 would be expected to display phenotypes that overlap with *5mCUC1* phenotypes. Therefore, we searched the Salk Institute Genomic Analysis Laboratory collection [46] for plants with disruptions in *MIR164a* and *MIR164b*, two genomic loci with the potential to encode miR164 [7]. Although no mutants were found with insertions near *MIR164a*, a mutant (designated *mir164b-1*) was found with a T-DNA insertion within the *MIR164b* foldback. Sequencing the left border junction revealed that the T-DNA was inserted in the loop of the predicted hairpin precursor. The reduced miR164 accumulation in this line (Figure 5A) indicated that it may be a *miR164b* null allele. Although the level of miR164 accumulation was reduced approximately 15-fold in *mir164b* mutant seedlings (Figure 5A), we did not observe any developmental abnormalities in the mutant plants, indicating that the reduction in miR164 level at this early developmental stage is not sufficient to impact development. In accordance with this result, quantitative RT-PCR analysis of miR164

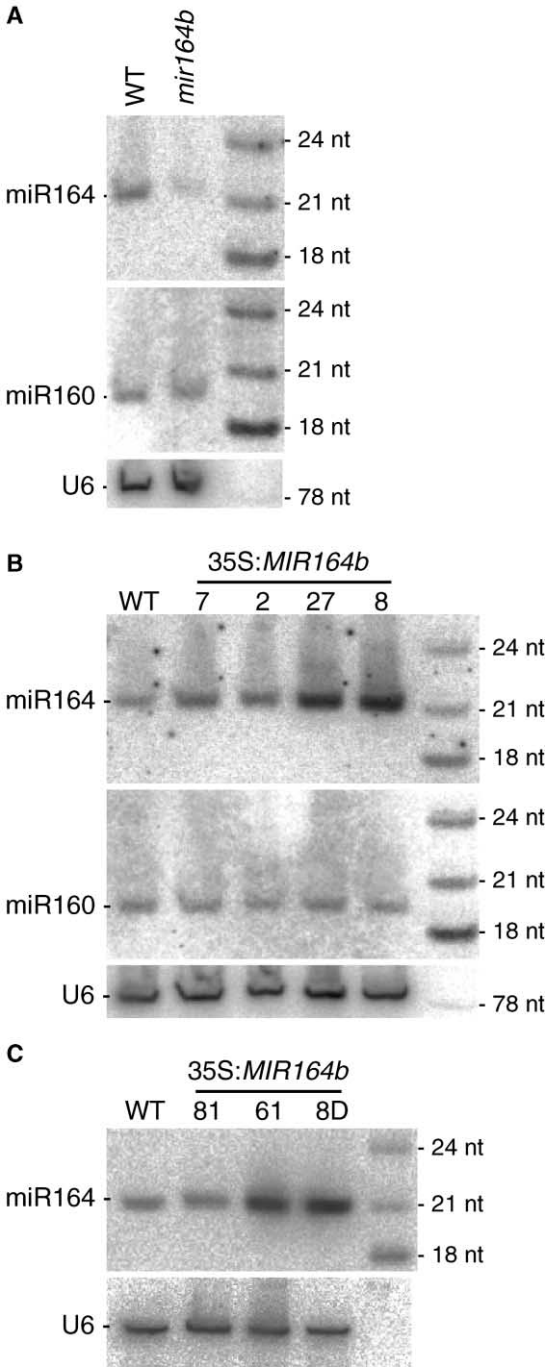


Figure 5. Reduced miR164 Accumulation *mir164b* Mutant Plants and Increased miR164 Levels in 35S:*MIR164b* Plants.

(A) RNA gel-blot analysis of 30 μg total RNA prepared from 7-day-old wt Col-0 and *mir164b-1* (SALK_136105) seedlings.

(B) Progeny of *35S:MIR164b* plants that display organ fusion phenotypes have increased seedling miR164 accumulation. RNA gel-blot analysis of 30 μg total RNA prepared from 7-day-old wt Col-0 seedlings and 7-day-old seedling progeny of *35S:MIR164b* plants. Line 7 displayed no fusion phenotypes; line 2 displayed stem-pedicle and weak sepal fusions; line 27 displayed stem-pedicle, stem-leaf, and sepal fusions; and line 8 displayed stem-pedicle, stem-leaf, sepal, stamen, and rosette leaf fusions.

(C) *35S:MIR164b* plants that display organ fusion phenotypes have increased miR164 accumulation in flowers. RNA gel-blot analysis of 9 μg total RNA prepared from a mix of buds and inflorescence meristems of wt Col-0 and *35S:MIR164b* plants. Line 81 displayed no fusion phenotypes; line 61 displayed stem-pedicle, stem-leaf, and sepal fusions; and line 8D displayed stem-pedicle, stem-leaf, sepal, stamen, and rosette leaf fusions. The positions of $^{32}$P-labeled RNA oligonucleotides are noted. Blots were stripped and reprobed with oligonucleotides complementary to miR160 and U6 as loading controls.

target mRNA levels in *mir164b* mutant seedlings did not reveal consistent changes in mRNA steady-state levels of the five predicted miR164 targets (data not shown). The T-DNA insertion in *miR164b-1* is located within the loop of the miR164b precursor; thus, it is likely that this line is a null allele and it supports the hypothesis that *MIR164a* is at least partially redundant with *MIR164b*. Interestingly, a miR164-like sequence (miR164c) was cloned from *Arabidopsis* that differs from the sequence of miR164a and miR164b by a single adenine-to-guanine substitution at the 3′ end (M. Jones-Rhoades, B. Reinhart, B.B., and D.P.B., unpublished data); therefore, miR164c may also contribute to miR164 target gene regulation.

### Constitutive Overexpression of *MIR164b* Recapitulates *cuc1 cuc2* Double Mutant Phenotypes

Because plants expressing a miR164-resistant *CUC1* mRNA have altered development, we expected that proper miR164 expression would also be required for normal development. To investigate this hypothesis, the stem loop of the *MIR164b* gene was cloned behind the CaMV 35S promoter and introduced into wt *Arabidopsis* plants. Misexpressed miR164 was expected to increase target mRNA cleavage, especially in cells that normally do not express the miRNA, and thereby phenocopy the organ separation defects seen in the *cuc1 cuc2* double mutants, including fused cotyledons, sepals, and stamens [40, 43]. Indeed, although most *35S:MIR164b* primary transformant seedlings had a wild-type appearance (Figures 6A and 6D), several displayed partially fused cotyledon petioles (Figures 6B and 6C), similar to the *cuc1 cuc2* mutants [40]. Mild cotyledon petiole fusion was correlated with the first true leaves appearing asymmetrically from the shoot apex (Figures 6E and 6F). More dramatic and frequent fusion phenotypes were observed in adult plants. 58 of 85 *35S:MIR164b* primary transformants displayed partial or complete sepal fusion (Figures 6Q and 6R; compare to Figures 6L and 6M), and 16 of 85 displayed some degree of stamen fusion (Figure 6S; compare to Figure 6N). These results demonstrate that misexpression of *MIR164b* can recapitulate certain *cuc1 cuc2* double mutant phenotypes, indicating that control of miR164 dosage and localization is necessary for proper *CUC* activity.

Other phenotypes displayed by *cuc1 cuc2* double mutants were not frequently observed in the *35S:MIR164b* plants. In particular, *cuc1 cuc2* mutants often display cotyledons fused along both margins accompanied by a missing SAM [40], whereas the partial cotyledon fusions that we observed in some *35S:MIR164b* plants (Figure 6B, C) were usually accompanied by an intact SAM (Figures 6E and 6F). We did observe one transformed plant with fused cotyledon petioles and lacking a SAM (Figure

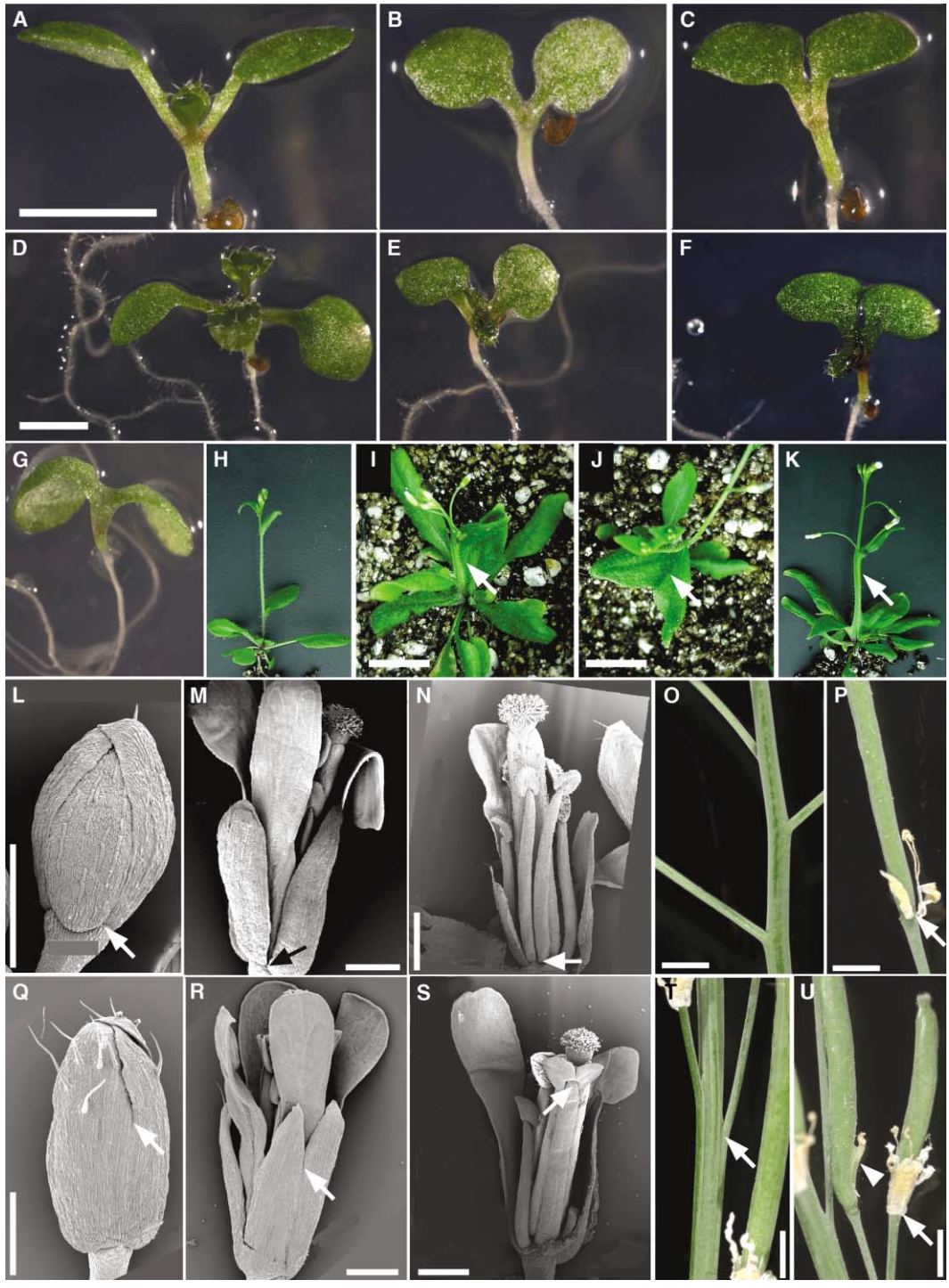


Figure 6. Fusion Phenotypes of *35S:MIR164b* Plants

(A–C) Ten-day-old *35S:MIR164b* seedlings displaying no fusion (A) or partial cotyledon petiole fusion (B and C).

(D–F) Same seedlings as in (A–C) at 13 days old, displaying true leaf formation to one side of the partially fused cotyledon petioles (E and F).

(G) 13-day-old *35S:MIR164b* seedling displaying fused cotyledon petioles and no SAM.

(H) 29-day-old wt Col-0 plant.

(I–K) *35S:MIR164b* plants (34 days old) displaying rosette leaf fusion (arrow in [J]) or leaf-stem fusions (arrows in [I] and [K]).

(L–P) Wild-type (Col-0) plants. Buds (L) and flowers (M) display separated sepals and six distinct stamen (N) imaged by SEM (arrows denote the points of separation). Pedicles emerge from the inflorescence stems (O) and separated flower parts abscise from the fertilized siliques (P).

(Q–U) *35S:MIR164b* T1 plants display floral organ fusion defects. Buds (Q) and flowers (R) have various extents of sepal fusion, and removal of sepals and petals exposes fused stamen ([S]; arrows denote points of separation). *35S:MIR164b* plants display varying degrees of pedicles fused to stems ([T]; arrow highlights the altered angles between pedicle and stem; compare to [O]). Fused sepals abscise late from *35S:MIR164b* siliques ([U]; arrow indicates dried sepals firmly attached to the silique). Occasional stamen-carpel fusions are observed (arrowhead in [U]). The scale bar in (A) represents 1 mm and applies to panels (A)–(C). The scale bar in (D) represents 1 mm and applies to panels (D)–(G). The scale bars in (I) and (J) represent 1 cm, the scale bars in (L)–(N) and (Q)–(S) represent 500 μm, and the scale bars in (O), (P), (T), and (U) represent 1 mm.

6G) among the 86 *35S:MIR164b* transformants observed. The reduced severity of embryonic defects in the *35S:MIR164b* plants compared to the *cuc1 cuc2* mutant may reflect the reduced activity of the 35S promoter during early stages of embryogenesis [47]. In addition, unlike *cuc1 cuc2* mutant plants, which lack functional CUC1 and CUC2 protein, *35S:MIR164b* plants still accumulate detectable levels of *CUC1* and *CUC2* mRNAs (data not shown).

### miR164-Directed Cleavage of *NAC1*, *At5g07680*, and *At5g61430* Could Explain Additional Organ-Separation Defects

Interestingly, *35S:MIR164b* plants display organ fusion phenotypes not reported in *cuc1 cuc2* mutants [40, 43, 44, 48]. These *35S:MIR164b* phenotypes include fused rosette leaves (13/85 T1 plants; Figure 6J), leaf-stem fusions (28/85 T1 plants; Figures 6I and 6K; compare to Figure 6H), stem-pedicle fusions (25/85 T1 plants; Figure 6T; compare to Figure 6O), and occasional stamen-silique fusions (Figure 6U). Floral organs of affected plants did not abscise normally after fertilization but, rather, remained on the parent plant (52/85 T1 plants; Figure 6U; compare to Figure 6P), perhaps due to sepal separation defects (Figures 6Q and 6R).

The organ separation defects in the *35S:MIR164b* plants that are not observed in *cuc1 cuc2* could be explained by miR164-directed cleavage of additional targets. In addition to *CUC1* and *CUC2*, at least three *Arabidopsis* NAC-domain genes, *NAC1*, *At5g07680*, and *At5g61430*, have extensive complementarity to miR164 ([25]; Figure 1A). To determine if these mRNAs are also targeted for cleavage in *Arabidopsis*, we amplified cleavage products from these mRNAs from wt *Arabidopsis* Col-0 RNA by using the RNA ligase-mediated 5′-RACE protocol that was used to demonstrate miR164-directed cleavage of *CUC1* and *CUC2* messages [28, 29]. RNA sequences with 5′ termini corresponding to the center of the miR164 complementary site were consistently detected for all three genes (Figure 1C), indicating that *NAC1*, *At5g07680*, and *At5g61430* are in vivo miR164 cleavage targets.

To assess whether the fusion phenotypes that we observed correlated with the level of miR164 overexpression, we examined miR164 levels in progeny seedlings of *35S:MIR164b* transformants with strong and weak fusion phenotypes. We found that progeny of plants with a variety of fusion defects accumulate miR164 to a level ~9-fold higher than wt, whereas progeny of *35S:MIR164b* plants without fusion phenotypes accumulated miR164 to a level similar to wt plants (Figure 5B). This correlation between miR164 levels and phenotypic severity was observed in RNA prepared from both seedlings (Figure 5B) and floral buds and meristems (Figure 5C), indicating that the miR164 overexpression persisted through development.

Together, our results strongly suggest that proper miR164-directed gene regulation of *CUC1*, *CUC2*, and at least one other NAC-domain gene is essential for the separation of adjacent embryonic, vegetative, and floral organs and implicate miR164 as a common regulatory factor in the mechanism(s) controlling organ separation.

The *cuc1 cuc2*–like fusions in *35S:MIR164b* plants (Figure 6), the increase in *CUC1* mRNA steady-state levels in *5mCUC1* plants with aberrant phenotypes (Figure 4), the detection of miR164-directed mRNA cleavage products in wild-type *Arabidopsis* (Figure 1), and the increase in *CUC2* mRNA accumulation in mutants defective in miRNA biogenesis and function [22], all suggest that miR164 is regulating its target genes, at least in part, by mediating mRNA cleavage. However, we cannot rule out the possibility that miR164, in addition to directing mRNA degradation, may also repress translation, as reported for miR172 [31, 32].

### miRNA Regulation of Lateral Organ Boundaries in Plants

miR164 is conserved between *Arabidopsis* and rice [7], and miR164 targets are found in the NAC-domain family in other plants as well. For example, rice encodes a NAC-domain mRNA (*OsNAC2*) with a two-mismatch miR164 complementary site [25]. In addition, examination of the petunia *NAM* [41] and snapdragon *CUPULIFORMIS* (*CUP*) mRNAs [49] reveals that each contain a miR164 complementarity site with three mismatches (Figure 1A). The petunia *nam* mutant displays cotyledon fusions and usually lacks a SAM [41]. *nam* shoots that develop display altered numbers of second and third whorl floral organ primordia [41]. The snapdragon *cup* mutant displays defects in SAM formation and dramatic cotyledon, leaf, inflorescence, and floral organ fusions [49] reminiscent of the diverse organ fusions observed in the *35S:MIR164b* plants (Figure 6). It is likely that several genes similar to *CUC1/2*, *NAM*, and *CUP* regulate lateral organ boundaries and that the exact division of labor among the genes varies depending upon the extent and nature of gene duplication in various plant lineages. The occurrence of miR164 complementary sites in these NAC-domain genes implicated in lateral organ boundary formation suggests that the miR164-based regulation of the process uncovered here will be general to flowering plants.

There are over 100 NAC-domain genes in *Arabidopsis*, but only some of these are known to be miR164 target genes. One miR164 target is *NAC1*, which is important in lateral root development; others are *Arabidopsis CUC1*, *CUC2*, *At5g07680*, and *At5g61430* (Figure 1C) [29]. Another likely miR164 target, *At5g39610*, which is closely related to *At5g07680* and *At5g61430*, has a miR164 complementarity site with only four mismatches (including one G:U wobble) and is among the miR164 targets predicted in a recent computational analysis (M. Jones-Rhoades and D.P.B., unpublished data). However, other closely related genes of unknown function (e.g., *At3g29035*) and *CUC3*, which has a function partially redundant with *CUC1* and *CUC2* [50], lack extensive complementarity to miR164. It appears that miR164 regulation of these genes has either been lost over the course of evolution or does not involve extensive complementarity between the miRNA and the messages.

In plants, organ primordia derive from stem cells in the meristematic regions. These pluripotent stem cells develop into determinate organs through a series of coordinated cell-cell signaling events [51]. During embryogenesis, *CUC1* and *CUC2* are expressed in a few

apical cells as early as the globular stage, and as the embryo develops, expression spreads to numerous cells located between the two cotyledon primordia [40, 43, 48]. This *CUC1* and *CUC2* expression is thought to define boundaries between developing cotyledons, perhaps by restricting cell proliferation, and thereby helping to establish bilateral symmetry [40, 43, 48]. *CUC1* and *CUC2* also are required for adjacent floral organ separation, suggesting that an analogous boundary definition process occurs during floral development [40, 43, 48], and our data point to other NAC-domain genes mediating additional organ separation events. The identification of miR164 as an integral regulator of a subset of NAC-domain genes, including *CUC1* and *CUC2*, adds a new layer of complexity to the gene regulatory mechanisms that control cell differentiation and organ development in plants.

Perturbing miR164-directed *CUC1* or *CUC2* regulation in the *5mCUC1* and *35S:MIR164b* plants would likely misregulate genes that rely directly or indirectly on proper *CUC1* or *CUC2* expression. For example, *CUC1* or *CUC2* is required for expression of *SHOOT MERISTEMLESS (STM)* [44, 48], which encodes a class I knotted-like homeobox (KNOX) protein that functions in meristematic and interprimordial regions to maintain cells in an undifferentiated state and to prevent these cells from proliferating [52–54]. Loss of STM results in partial cotyledon and floral organ fusions and reduced or absent SAM formation, reminiscent of the defects in *35S:MIR164b* plants (Figure 6) [54, 55]. Genetic interactions imply that *STM* maintains the SAM by inhibiting expression of *ASYMMETRIC LEAVES1 (AS1)*, a MYB-domain transcription factor [56]. *as1* mutants develop abnormal rosette leaves with outgrowths or lobes [56], a phenotype similar to that of *5mCUC1* plants (Figures 3B and 3C). Thus, misexpression of genes known to be downstream of *CUC1* or *CUC2* is likely to contribute to the cotyledon, leaf, and floral organ defects that we observed (Figures 3 and 6).

Interestingly, the phenotypes observed in the *5mCUC1* plants did not overlap with phenotypes reported for *35S:CUC1* plants, which include lobed cotyledons and ectopic adaxial meristems [43, 44]. The CaMV 35S promoter likely directs higher and more widespread expression than the *CUC1* promoter [57], and thus miR164 may not be at sufficient levels in all relevant tissues to counter the message expressed in *35S:CUC1* plants, even though miR164 is present in many organs (Figure 2B). Similarly, plants expressing *35S:NAC1* also have developmental abnormalities [45]. The fact that 35S promoter-driven expression of *CUC1* and *NAC1* confers developmental anomalies indicates that miRNA-mediated regulation and other forms of posttranscriptional control, such as ubiquitin-mediated proteolysis [58], may not be sufficient for proper development and suggests that transcriptional regulation of both genes is also necessary. Indeed, *CUC1* transcriptional control was demonstrated when in situ hybridization analysis of embryonic *CUC1* mRNA accumulation [43] showed *CUC1* expression closely resembling the embryonic pattern of *CUC1* promoter-driven green fluorescent protein (GFP) accumulation [57], even though the GFP reporter does not contain a miR164 complementary site. Nonetheless, the cotyledon orientation defects observed in *5mCUC1* plants (Figure 3A) reveal a clear role for miR164 during embryonic development that may be too subtle to detect by comparing mRNA in situ analysis with that of GFP reporters, suggesting that miRNAs also may be playing roles in other cases where posttranscriptional regulation has not been suspected. The striking abnormalities observed during floral development of *5mCUC1* plants (Figure 3) also illustrate the importance of miRNA-mediated postembryonic regulation of *CUC1*. Notably, the dual control of *CUC1* and *NAC1* by both transcriptional and posttranscriptional mechanisms distinguishes these miR164 targets from several mRNAs targeted by the miR156/157, miR159/JAW, miR165/166, and miR172 families, which do not confer dramatic phenotypes when driven by the 35S promoter but, in the cases tested, do confer dramatic phenotypes when miRNA-resistant versions are expressed [26, 32, 38, 59].

Petal and sepal whorls have different responses to the increased or expanded presence of the *5mCUC1* miR164-resistant mRNA, perhaps reflecting somewhat differing gene regulatory circuitry controlling the separation of developing petal and sepal primordia. We speculate that the increased number of petals and decreased number of sepals could both be the outcome of increased organ separation in these plants: in one case increased instances of separation and in the other, an increased degree of separation. In the petal whorl, loss of miR164-mediated *CUC1* regulation may increase the instances of petal primordia separation, resulting in additional primordia, and ultimately additional petals. In the sepal whorl, loss of miR164-mediated *CUC1* regulation may increase the degree of separation between sepal primordia, resulting in fewer sepal primordia. The discovery that miR164-directed mRNA cleavage is important in these processes of organ development and separation will facilitate their molecular characterization.

## Conclusions

Here, we demonstrate that miR164 regulates NAC-domain target genes in *Arabidopsis*. Perturbation of miR164-directed regulation causes development abnormalities in embryonic, vegetative, and floral organs, thus establishing miR164 as a key regulatory component essential for normal plant development and furthering the understanding of the biological roles of miRNA regulation in plants.

## Experimental Procedures

### DNA Constructs and Transgenic Plants

#### *CUC1* and *5mCUC1*

The genomic sequence of *CUC1* (At3g15170), including ~1.4 kilobases (kb) and ~0.7 kb of putative 5′ and 3′ regulatory sequences, respectively, was cloned as an ~3.7 kb BamH1-EcoR1 fragment into pBluescriptIISK+ (Stratagene) from the bacterial artificial chromosome F4B12. Site-directed mutagenesis was performed by using *PfuUltra* polymerase followed by Dpn1 digestion, as suggested by the manufacturer (Stratagene), to produce the *5mCUC1* sequence. The sequence of the primer pair used for *CUC1* mutagenesis is *5mCUC1* forward 5′-CCGATCATCAATACCTTTGCGACGGAGCATGTTTCATGTTTTT CAAATAACTCTGCTGCTCATACCG-3′ and *5mCUC1* reverse 5′-CGGTATGAGCAGCAGAGTTATTTGAAAAACATGAAACATGCTCCGTCGCAAAGGTATTGATGATCGG-3′. After mutagenesis, a 1.5 kb Pac1-Nco1 fragment spanning the mutagenized *CUC1*

miR164 complementary site was subcloned and used to replace the corresponding wild-type sequence of the original genomic *CUC1* clone. This 1.5 kb fragment was sequenced to ensure that only the desired silent mutations were present. The control *CUC1* and the *5mCUC1* ~3.7 kb BamH1-EcoR1 fragments were subcloned into the binary vector pGreenII0219 and then electroporated [60] into *Agrobacterium tumefaciens* strain GV3101::pMP90 [61]. *Arabidopsis thaliana* (Col-0 accession) was transformed by using the floral dip method [62]. The collected seeds were surface sterilized and plated on Bouturage No. 2 media (Duchefa Biochemie) containing 30 μg/mL hygromycin for selection of transformants. Seedlings were grown under long-day conditions (16 hr light, 8 hr dark) at 20°C for about 14 days before transfer to Metromix 200 soil (Scotts), where they were grown at 20°C under long-day conditions.

***35S:MIR164b***

To make the *35S:MIR164b* construct, genomic DNA from Col-0 plants was PCR amplified by using oligonucleotides MIR164b-C3 5′-GTCctcgagTCACGTTTTCAAATATCAAACCTAC-3′ and MIR164b-C2 5′-TATgcggccgcTCTCCTGTCTAATACTCGCTAACC-3′, which have flanking Xho1 or Not1 sites (lowercase). The resulting ~900 basepair (bp) product encoded the predicted miR164b hairpin precursor along with 385 bp of upstream and 355 bp of downstream sequence. The PCR amplification product was gel purified by using a Matrix Gel Extraction kit (Marligen Biosciences, Ijamsville, MD) and subcloned into the pCR4-TOPO vector (Invitrogen). The resultant clones were sequenced to identify PCR-derived errors, and a clone was selected with the expected sequence except for an A and T deleted 374 bp and 192 bp upstream of the foldback, respectively. The XhoI-NotI insert from this clone was ligated into Xho1-Not1-cut 35SpBARN [63] between the CaMV 35S promoter and the *nos* terminator. The resultant *35S:MIR164b* plasmid was electroporated [60] into *A. tumefaciens* GV3101, which was used to transform Col-0 by using the floral dip method [62]. Transformants were identified on PN (plant nutrient medium) [64] plates containing 7.5 μg/ml glufosinate ammonium (Crescent Chemical, Augsburg, Germany). Seedlings were grown under continuous light at 22°C for approximately 14 days before transfer to Metromix 200 soil (Scotts), where they were grown in continuous light at 22°C. Transformation of each T1 plant was confirmed by PCR amplification of genomic DNA [65] with the primers 35S-F 5′-AAGGGATGACGCACAATCCCACTATCC-3′ and MIR164b-C2, which yielded a 1 kb product from Col-0 (*35S:MIR164b*) plants.

***mir164b***

The *mir164b* mutant was identified from the SALK_136105 line generated by the SALK Institute Genomic Analysis Laboratory, La Jolla, CA [46]. The genotypes of plants segregating for this insertion obtained from the ABRC were determined by PCR-amplifying genomic DNA by using the primers MIR164b-1 5′-CAAAGAAATGTTGTTACC TGGTAATTAG-3′ and a modified version of the LBb1 primer 5′-CAAACCAGCGTGGACCGCTTGCTGCAACTC-3′; http://signal.salk.edu), which results in an ~700 bp product from the disrupted chromosome, or MIR164b-1 and MIR164b-4 5′-CCATAAAGCTTCAAAA TTTACAGAGTTTCC-3′, which results in a 694 bp product from the wild-type chromosome. The former product was directly sequenced by using the LBb1 primer to determine the exact location of the T-DNA insert, which was found to be at position 84 within the 149 nt predicted foldback of *MIR164b*. Homozygous plants were compared to the wild-type Col-0 after growth on PN medium supplemented with 0.5% sucrose or in soil.

### *CUC1* Transcript Preparation and In Vitro Cleavage Assay

*Arabidopsis CUC1* transcripts containing the miR164 complementary site were generated by PCR amplification of *CUC1* or *5mCUC1* genomic clones followed by in vitro transcription by using T7 RNA polymerase. The primer sequences used to generate *CUC1* and *5mCUC1* template were 5′-GGCCGTAATACGACTCACTATAGGGG AGAAGGAGTGGTACTTCTTC-3′ and 5′-CATTGCAAATGACGGAGG AGG-3′. Wheat germ lysate preparation, cap labeling, and in vitro cleavage assays were performed as described [30].

### 5′ RACE

poly(A)$^+$ RNA isolation, cDNA synthesis, non-gene-specific 5′-RACE amplifications, and gene-specific 5′-RACE amplifications were performed as described [28, 29] by using the GeneRacer Kit (Invitrogen) with the exception that an additional nested gene-specific 5′-RACE amplification was performed. The following primers were used with the GeneRacer 5′ Nested Primer: *NAC1* external 5′-CAGTGCTTG GAATACCGATGTCGGTCAG-3′, *NAC1* internal 5′-GCTGACTGAG TAGAGCTCTGAGAACCATC-3′; *At5g61430* external 5′-GATCAACC GGTCCAGTAGAGGAAGACGG-3′, *At5g61430* internal 5′-CAGTGT TCATGTCAGTTGAAACTCCGG-3′; *At5g07680* external 5′-GGTTCA AGATCAACCGGACCGGAAGAG-3′, *At5g07680* internal 5′-CCCGGT TTCTTGCGAGATGC TCAATG-3′.

### RNA Isolation and miRNA Gel-Blot Analysis

Total RNA was isolated as described [66] or by using RNeasy Plant Mini Kits (Qiagen, Valencia, CA). For RNA gel-blot analysis, total RNA was separated on a 15% denaturing polyacrylamide gel, electroblotted to nylon membrane, and hybridized with an end-labeled miR164 DNA probe, and then stripped and reprobed with miR160 and/or U6 DNA probes [7]. Hybridization signals were quantified with a Fuji phosphorimager.

### Reverse Transcription and Quantitative Real-Time PCR

For each sample, 0.6 μg total RNA was treated with DNaseI (Amplification Grade, Roche Applied Science, Indianapolis, IN) and reverse transcribed in a 40 μl volume by using 400 units SuperScript III (Invitrogen, Carlsbad, CA) primed with a mixture of reverse primers (QRTR primers listed below; 2 μM each) for the NAC-domain genes, *TUB4*, and 18S rRNA. The resulting cDNA was diluted to 200 μl with water. Gene-specific primers and TaqMan probes were designed to span the miRNA-complementary site of each mRNA by using Primer Express software (Applied Biosystems, Foster City, CA). Quantitative real-time PCR was carried out in triplicate 25 μl reactions by using the ABI Prism 7000 Sequence Detection System and TaqMan Universal PCR Master Mix (ABI) with primers at a final concentration of 0.5 μM each and using 10 μl diluted cDNA for the mRNAs or 0.001 μl for the 18S reaction. Primer pairs used were CUC1-QRTF 5′-TCTGCCGGTTCTGCAATTG-3′ and CUC1-QRTR 5′-CATCGGTATGAGCAGCAGAGTT-3′, CUC2-QRTF 5′-CAGCCGT AGCACCAACACAA-3′ and CUC2-QRTR 5′-GTCTAAGCCCAAGGCC CCGTAGTA-3′, NAC1-QRTF 5′-AACCCTCTTCTTATCTCAGTGATG ATC-3′ and NAC1-QRTR 5′-AGGTTCGAGTTTAAGGTTTGGTTCT-3′, At5g07680-QRTF 5′-CCACCTTTAACTGATTCTTCACCATA-3′, and At5g07680-QRTR 5′-AGCAATTGAGTATTGTTCCTCTAGTT TCA-3′, At5g61430-QRTF 5′-CCAAAACAGAACCGGTCTACGT-3′ and At5g61430-QRTR 5′-GAAGCAATTGAGTGTGGTTCCTT-3′, TUB4-QRTF 5′-CTGTTTCCGTACCCTCAAGC-3′, and TUB4-QRTR 5′-AGG GAAACGAAGACAGCAAG-3′. The following probes were paired with the respective primer pairs at a final concentration of 0.2 μM: CUC1-probe 5′-TCCGATCATCAATACCT-3′, CUC2-probe 5′-AGCGCAA TAACCGAGC-3′, NAC1-probe 5′-CTACATCATCAATGAGCA-3′, At5g-probe 5′-CTGCTTCTCCAACCAA-3′, and TUB4-probe 5′-CGCTAAT CCTACCTTTGGTGATCTTAACCAT-3′. The NAC-domain gene specific probes were 5′ labeled with 6-FAM and 3′ labeled with MGBNFQ (minor groove binder/nonfluorescent quencher). The TUB4 probe was 5′ labeled with HEX and 3′ labeled with TAMRA. The 18S primers and probe were from ABI (TaqMan Ribosomal RNA Control Reagents). PCR conditions were 2 min at 50°C and 10 min at 95°C followed by 40 cycles of 95°C for 15 s and 60°C for 1 min. cDNA amplification was monitored in real time by using ABI Prism 7000 Sequence Detection System software. Amplification of 18S rRNA was monitored as an endogenous control that was used to normalize template amounts using the comparative $C_T$ method (ABI Prism 7700 Sequence Detection System User Bulletin #2, http://www.appliedbiosystems.com). Control reactions in which reverse transcriptase was omitted did not give amplification signals above the threshold. Direct sequencing of the *CUC1* and *CUC2* amplification products revealed that the *CUC1* and *CUC2* primer pairs were gene specific.

### RT-PCR, Nsp1 Digestion, and DNA Gel-Blot Analysis

Total RNA was prepared from a mix of buds and inflorescence meristems of 57-day-old T2 *5mCUC1*, control *CUC1*, and wt Col-0 plants as described [66]. 5 μg of total RNA was used for oligo-$(dT)_{20}$ primed first strand cDNA synthesis followed by RNase H digestion as recommended by the manufacturer (ThermoScript RT system,

Invitrogen). PCR amplification with 50 ng of cDNA as a template was performed to completion by using the following *CUC1* primer pair: *CUC1* forward 5′-GCGTAGTTAGTAGAGAGACG-3′ and *CUC1* reverse 5′-GAGGCAGAGAAGGTAGATTCG-3′. To equalize the possibility of heteroduplex formation in the *5mCUC1* samples, the final PCR products were denatured and renatured. Nsp1 digestion of the 330 bp *5mCUC1* PCR product yielded ~110 bp and ~220 bp fragments. The wt *CUC1* PCR product did not contain an Nsp1 restriction site and thus was not cleaved after Nsp1 digestion. To monitor Nsp1 digestion efficiency, parallel reactions were conducted in which each reaction was spiked with a 1.2 kb DNA fragment containing an Nsp1 restriction site, which produced ~560 bp and ~600 bp fragments after digestion. This control DNA was cleaved to completion, indicating that the undigested fragments in the *5mCUC1* RT-PCR did not contain the Nsp1 site and derived from the endogenous *CUC1* gene. DNA gel-blot analysis was performed as described [66]. Undigested and Nsp1-digested PCR amplified products were separated on a 2% agarose gel, blotted to nylon membrane, and hybridized with $^{32}$P end-labeled *CUC1* reverse primer (above), which detects both the undigested *CUC1* and *5mCUC1* 330 bp PCR products and the 220 bp fragment generated by Nsp1 digestion of the *5mCUC1* PCR product. Hybridization signals were quantified with a Fuji phosphorimager. Heteroduplex DNA involving one strand of *CUC1* hybridized to one strand of *5mCUC1* was assumed to be refractory to Nsp1 cleavage. The square root of the fraction cut by Nsp1 indicated the total fraction of *5mCUC1* present as either a homoduplex or one strand of a heteroduplex and was used to calculate the reported mRNA ratios.

### Scanning Electron Microscopy

Plant tissues were fixed in 3% gluturaldehyde, 25 mM $NaPO_4$ (pH 6.8) overnight at 4°C with constant shaking, rinsed five times with 50 mM sodium cacodylate buffer (pH 7.0), and treated with 1% $OsO_4$, 50 mM sodium cacodylate (pH 7.0) for at least 6 hours at 25°C. Tissues were dehydrated through a graded ethanol series (25%, 50%, 75%, 90%, 95%, and 100% ethanol) and then critical point dried by using $CO_2$. Tissues were mounted on stubs and shadowed with gold and pallidium (4:1) before viewing through a Jeol 5600LV scanning electron microscope.

### Acknowledgments

We thank M. Jones-Rhoades, G. Tang, and P. Zamore for wheat germ extracts; M. Axtell for cDNA used in the RNA ligase-mediated 5′ RACE reactions; P. Mullineaux and R. Hellens (John Innes Centre and The Biotechnology and Biological Sciences Research Council) for the pGreenII0129 binary vector; M.E. Lane for microscope use; and N. Watson of the W.M. Keck Foundation Biological Imaging Facility at the Whitehead Institute for scanning electron microscopy technical advice. The Salk Institute Genomic Analysis Laboratory generated the sequence-indexed T-DNA insertion mutant (*mir164b*), and the *Arabidopsis* Biological Resource Center at Ohio State University supplied *mir164b* seeds and the F4B12 clone. We thank H. Vaucheret and members of each Bartel laboratory for helpful advice and critical comments on the manuscript. This research was supported by the National Institutes of Health (F32-GM071200, A.C.M.; T32-GM08362, D.V.D.; R24-GM069512, B.B. and D.P.B.), the G. Harold and Leila Y. Mathers Charitable Foundation (B.B.), the Robert A. Welch Foundation (C-1309, B.B.), and the Alexander and Margaret Stewart Trust (D.P.B.).

Received: March 18, 2004
Revised: April 13, 2004
Accepted: April 19, 2004
Published: June 22, 2004

### References

1. Bartel, D.P. (2004). MicroRNAs: genomics, biogenesis, mechanism, and function. Cell *116*, 281–297.
2. Lee, R.C., Feinbaum, R.L., and Ambros, V. (1993). The *C. elegans* heterochronic gene *lin-4* encodes small RNAs with antisense complementarity to *lin-14*. Cell *75*, 843–854.
3. Reinhart, B.J., Slack, F.J., Basson, M., Pasquinelli, A.E., Bettinger, J.C., Rougvie, A.E., Horvitz, H.R., and Ruvkun, G. (2000). The 21-nucleotide let-7 RNA regulates developmental timing in *Caenorhabditis elegans*. Nature *403*, 901–906.
4. Lagos-Quintana, M., Rauhut, R., Lendeckel, W., and Tuschl, T. (2001). Identification of novel genes coding for small expressed RNAs. Science *294*, 853–858.
5. Lau, N.C., Lim, L.P., Weinstein, E.G., and Bartel, D.P. (2001). An abundant class of tiny RNAs with probable regulatory roles in *Caenorhabditis elegans*. Science *294*, 858–862.
6. Lee, R.C., and Ambros, V. (2001). An extensive class of small RNAs in *Caenorhabditis elegans*. Science *294*, 862–864.
7. Reinhart, B.J., Weinstein, E.G., Rhoades, M.W., Bartel, B., and Bartel, D.P. (2002). MicroRNAs in plants. Genes Dev. *16*, 1616–1626.
8. Llave, C., Kasschau, K.D., Rector, M.A., and Carrington, J.C. (2002). Endogenous and silencing-associated small RNAs in plants. Plant Cell *14*, 1605–1619.
9. Park, W., Li, J., Song, R., Messing, J., and Chen, X. (2002). CARPEL FACTORY, a Dicer homolog, and HEN1, a novel protein, act in microRNA metabolism in *Arabidopsis thaliana*. Curr. Biol. *12*, 1484–1495.
10. Wightman, B., Ha, I., and Ruvkun, G. (1993). Posttranscriptional regulation of the heterochronic gene *lin-14* by *lin-4* mediates temporal pattern formation in *C. elegans*. Cell *75*, 855–862.
11. Brennecke, J., Hipfner, D.R., Stark, A., Russell, R.B., and Cohen, S.M. (2003). *bantam* encodes a developmentally regulated microRNA that controls cell proliferation and regulates the proapoptotic gene *hid* in *Drosophila*. Cell *113*, 25–36.
12. Johnston, R.J., and Hobert, O. (2003). A microRNA controlling left/right neuronal asymmetry in *Caenorhabditis elegans*. Nature *426*, 845–849.
13. Stark, A., Brennecke, J., Russell, R.B., and Cohen, S.M. (2003). Identification of *Drosophila* microRNA targets. PLoS Biol. 1(3): e60 DOI:10.1371/journal.pbio.0000060.
14. Lewis, B.P., Shih, I., Jones-Rhoades, M.W., Bartel, D.P., and Burge, C.B. (2003). Prediction of mammalian microRNA targets. Cell *115*, 787–798.
15. Yekta, S., Shih, I., and Bartel, D.P. (2004). MicroRNA-directed cleavage of *HOXB8* mRNA. Science *304*, 594–596.
16. Bartel, B., and Bartel, D.P. (2003). MicroRNAs: at the root of plant development? Plant Physiol. *132*, 709–717.
17. Papp, I., Mette, M.F., Aufsatz, W., Daxinger, L., Schauer, S.E., Ray, A., van der Winden, J., Matzke, M., and Matzke, A.J. (2003). Evidence for nuclear processing of plant micro RNA and short interfering RNA precursors. Plant Physiol. *132*, 1382–1390.
18. Boutet, S., Vazquez, F., Liu, J., Béclin, C., Fagard, M., Gratias, A., Morel, J.B., Crété, P., Chen, X., and Vaucheret, H. (2003). *Arabidopsis HEN1*: A genetic link between endogenous miRNA controlling development and siRNA controlling transgene silencing and virus resistance. Curr. Biol. *13*, 843–848.
19. Vazquez, F., Gasciolli, V., Crete, P., and Vaucheret, H. (2004). The nuclear dsRNA binding protein HYL1 is required for microRNA accumulation and plant development, but not posttranscriptional transgene silencing. Curr. Biol. *14*, 346–351.
20. Han, M.H., Goud, S., Song, L., and Fedoroff, N. (2004). The *Arabidopsis* double-stranded RNA-binding protein HYL1 plays a role in microRNA-mediated gene regulation. Proc. Natl. Acad. Sci. USA *101*, 1093–1098.
21. Kidner, C.A., and Martienssen, R.A. (2004). Spatially restricted microRNA directs leaf polarity through ARGONAUTE1. Nature *428*, 81–84.
22. Vaucheret, H., Vazquez, F., Crété, P., and Bartel, D.P. (2004). The action of *ARGONAUTE1* in the miRNA pathway and its regulation by the miRNA pathway are crucial for plant development. Genes Dev. *18*, 1187–1197.
23. Carmell, M.A., Xuan, Z., Zhang, M.Q., and Hannon, G.J. (2002). The Argonaute family: tentacles that reach into RNAi, developmental control, stem cell maintenance, and tumorigenesis. Genes Dev. *16*, 2733–2742.
24. Floyd, S.K., and Bowman, J.L. (2004). Ancient microRNA target sequences in plants. Nature *428*, 485–486.
25. Rhoades, M.W., Reinhart, B.J., Lim, L.P., Burge, C.B., Bartel,

B., and Bartel, D.P. (2002). Prediction of plant microRNA targets. Cell *110*, 513–520.
26. Palatnik, J.F., Allen, E., Wu, X., Schommer, C., Schwab, R., Carrington, J.C., and Weigel, D. (2003). Control of leaf morphogenesis by microRNAs. Nature *425*, 257–263.
27. Xie, Z., Kasschau, K.D., and Carrington, J.C. (2003). Negative feedback regulation of *Dicer-like1* in *Arabidopsis* by microRNA-guided mRNA degradation. Curr. Biol. *13*, 784–789.
28. Llave, C., Xie, Z., Kasschau, K.D., and Carrington, J.C. (2002). Cleavage of *Scarecrow-like* mRNA targets directed by a class of *Arabidopsis* miRNA. Science *297*, 2053–2056.
29. Kasschau, K.D., Xie, Z., Allen, E., Llave, C., Chapman, E.J., Krizan, K.A., and Carrington, J.C. (2003). P1/HC-Pro, a viral suppressor of RNA silencing, interferes with *Arabidopsis* development and miRNA function. Dev. Cell *4*, 205–217.
30. Tang, G., Reinhart, B.J., Bartel, D.P., and Zamore, P.D. (2003). A biochemical framework for RNA silencing in plants. Genes Dev. *17*, 49–63.
31. Aukerman, M.J., and Sakai, H. (2003). Regulation of flowering time and floral organ identity by a microRNA and its *APETALA2*-like target genes. Plant Cell *15*, 2730–2741.
32. Chen, X. (2004). A microRNA as a translational repressor of *APETALA2* in *Arabidopsis* flower development. Science *303*, 2022–2025.
33. Robinson-Beers, K., Pruitt, R.E., and Gasser, C.S. (1992). Ovule development in wild-type Arabidopsis and two female-sterile mutants. Plant Cell *4*, 1237–1249.
34. Jacobsen, S.E., Running, M.P., and Meyerowitz, E.M. (1999). Disruption of an RNA helicase/RNAse III gene in *Arabidopsis* causes unregulated cell division in floral meristems. Development *126*, 5231–5243.
35. Chen, X., Liu, J., Cheng, Y., and Jia, D. (2002). HEN1 functions pleiotropically in Arabidopsis development and acts in C function in the flower. Development *129*, 1085–1094.
36. Schauer, S.E., Jacobsen, S.E., Meinke, D.W., and Ray, A. (2002). *DICER-LIKE1*: blind men and elephants in *Arabidopsis* development. Trends Plant Sci. *7*, 487–491.
37. Mallory, A.C., Reinhart, B.J., Bartel, D., Vance, V.B., and Bowman, L.H. (2002). A viral suppressor of RNA silencing differentially regulates the accumulation of short interfering RNAs and micro-RNAs in tobacco. Proc. Natl. Acad. Sci. USA *99*, 15228–15233.
38. Emery, J.F., Floyd, S.K., Alvarez, J., Eshed, Y., Hawker, N.P., Izhaki, A., Baum, S.F., and Bowman, J.L. (2003). Radial patterning of *Arabidopsis* shoots by class III HD-ZIP and KANADI genes. Curr. Biol. *13*, 1768–1774.
39. Juarez, M.T., Kui, J.S., Thomas, J., Heller, B.A., and Timmermans, M.C. (2004). microRNA-mediated repression of *rolled leaf1* specifies maize leaf polarity. Nature *428*, 84–88.
40. Aida, M., Ishida, T., Fukaki, H., Fujisawa, H., and Tasaka, M. (1997). Genes involved in organ separation in Arabidopsis: an analysis of the *cup-shaped cotyledon* mutant. Plant Cell *9*, 841–857.
41. Souer, E., van Houwelingen, A., Kloos, D., Mol, J., and Koes, R. (1996). The *no apical meristem* gene of Petunia is required for pattern formation in embryos and flowers and is expressed at meristem and primordia boundaries. Cell *85*, 159–170.
42. Riechmann, J.L., Heard, J., Martin, G., Reuber, L., Jiang, C., Keddie, J., Adam, L., Pineda, O., Ratcliffe, O.J., Samaha, R.R., et al. (2000). Arabidopsis transcription factors: genome-wide comparative analysis among eukaryotes. Science *290*, 2105–2110.
43. Takada, S., Hibara, K., Ishida, T., and Tasaka, M. (2001). The *CUP-SHAPED COTYLEDON1* gene of *Arabidopsis* regulates shoot apical meristem formation. Development *128*, 1127–1135.
44. Hibara, K., Takada, S., and Tasaka, M. (2003). *CUC1* gene activates the expression of SAM-related genes to induce adventitious shoot formation. Plant J. *36*, 687–696.
45. Xie, Q., Frugis, G., Colgan, D., and Chua, N.H. (2000). *Arabidopsis* NAC1 transduces auxin signal downstream of TIR1 to promote lateral root development. Genes Dev. *14*, 3024–3036.
46. Alonso, J.M., Stepanova, A.N., Leisse, T.J., Kim, C.J., Chen, H., Shinn, P., Stevenson, D.K., Zimmerman, J., Barajas, P., Cheuk, R., et al. (2003). Genome-wide insertional mutagenesis of *Arabidopsis thaliana*. Science *301*, 653–657.
47. Sunilkumar, G., Mohr, L., Lopata-Finch, E., Emani, C., and Rathore, K.S. (2002). Developmental and tissue-specific expression of CaMV 35S promoter in cotton as revealed by GFP. Plant Mol. Biol. *50*, 463–474.
48. Aida, M., Ishida, T., and Tasaka, M. (1999). Shoot apical meristem and cotyledon formation during Arabidopsis embryogenesis: interaction among the *CUP-SHAPED COTYLEDON* and *SHOOT MERISTEMLESS* genes. Development *126*, 1563–1570.
49. Weir, I., Lu, J., Cook, H., Causier, B., Schwarz-Sommer, Z., and Davies, B. (2004). *CUPULIFORMIS* establishes lateral organ boundaries in *Antirrhinum*. Development *131*, 915–922.
50. Vroemen, C.W., Mordhorst, A.P., Albrecht, C., Kwaaitaal, M.A., and de Vries, S.C. (2003). The *CUP-SHAPED COTYLEDON3* gene is required for boundary and shoot meristem formation in Arabidopsis. Plant Cell *15*, 1563–1577.
51. Baurle, I., and Laux, T. (2003). Apical meristems: the plant's fountain of youth. Bioessays *25*, 961–970.
52. Barton, M.K., and Poethig, R.S. (1993). Formation of the shoot apical meristem in *Arabidopsis thaliana*-an analysis of development in the wild type and in the *shoot meristemless* mutant. Development *119*, 823–831.
53. Clark, S.E., Jacobsen, S.E., Levin, J.Z., and Meyerowitz, E.M. (1996). The CLAVATA and SHOOT MERISTEMLESS loci competitively regulate meristem activity in Arabidopsis. Development *122*, 1567–1575.
54. Long, J.A., Moan, E.I., Medford, J.I., and Barton, M.K. (1996). A member of the KNOTTED class of homeodomain proteins encoded by the STM gene of Arabidopsis. Nature *379*, 66–69.
55. Endrizzi, K., Moussian, B., Haecker, A., Levin, J.Z., and Laux, T. (1996). The SHOOT MERISTEMLESS gene is required for maintenance of undifferentiated cells in Arabidopsis shoot and floral meristems and acts at a different regulatory level than the meristem genes WUSCHEL and ZWILLE. Plant J. *10*, 967–979.
56. Byrne, M.E., Barley, R., Curtis, M., Arroyo, J.M., Dunham, M., Hudson, A., and Martienssen, R.A. (2000). Asymmetric leaves1 mediates leaf patterning and stem cell function in Arabidopsis. Nature *408*, 967–971.
57. Cary, A.J., Che, P., and Howell, S.H. (2002). Developmental events and shoot apical meristem gene expression patterns during shoot development in *Arabidopsis thaliana*. Plant J. *32*, 867–877.
58. Xie, Q., Guo, H.-S., Dallman, G., Fang, S., Weissman, A.M., and Chua, N.-H. (2002). SINAT5 promotes ubiquitin-related degradation of NAC1 to attenuate auxin signals. Nature *419*, 167–170.
59. Cardon, G., Hohmann, S., Klein, J., Nettesheim, K., Saedler, H., and Huijser, P. (1999). Molecular characterisation of the Arabidopsis SBP-box genes. Gene *237*, 91–104.
60. Ausubel, F.M., Brent, R., Kingston, R.E., Moore, D.D., Seidman, J.G., Smith, J.A., and Struhl, K. (1995). Short Protocols in Molecular Biology, Third Edition (John Wiley & Sons, Inc.).
61. Koncz, C., and Schell, J. (1986). The promoter of the $T_L$-DNA gene 5 controls the tissue-specific expression of chimaeric genes carried by a novel type of *Agrobacterium* binary vector. Mol. Gen. Genet. *204*, 383–396.
62. Clough, S.J., and Bent, A.F. (1998). Floral dip: a simplified method for *Agrobacterium*-mediated transformation of *Arabidopsis thaliana*. Plant J. *16*, 735–743.
63. LeClere, S., and Bartel, B. (2001). A library of Arabidopsis 35S-cDNA lines for identifying novel mutants. Plant Mol. Biol. *46*, 695–703.
64. Haughn, G.W., and Somerville, C. (1986). Sulfonylurea-resistant mutants of *Arabidopsis thaliana*. Mol. Gen. Genet. *204*, 430–434.
65. Celenza, J.L., Grisafi, P.L., and Fink, G.R. (1995). A pathway for lateral root formation in *Arabidopsis thaliana*. Genes Dev. *9*, 2131–2142.
66. Mallory, A.C., Ely, L., Smith, T.H., Marathe, R., Anandalakshmi, R., Fagard, M., Vaucheret, H., Pruss, G., Bowman, L., and Vance, V.B. (2001). HC-Pro suppression of transgene silencing eliminates the small RNAs but not transgene methylation or the mobile signal. Plant Cell *13*, 571–583.

**Note Added in Proof**

The data referred to as "M. Jones-Rhoades and D.P.B., unpublished data" are now in press: Jones-Rhoades, M.W. and Bartel, D.P. (2004). Computational identification of plant microRNAs and their targets, including a stress-induced miRNA. Mol. Cell *14*, 787–799.